

## MONTE-CARLO SIMULATION RESULTS IN ESTIMATING A PURE-JUMP COX-INGERSOLL-ROSS PROCESS

ELISE BAYRAKTAR<sup>1</sup>

**Abstract.** We consider a pure-jump stable Cox-Ingersoll-Ross ( $\alpha$ -stable CIR) process driven by a non-symmetric stable Lévy process with jump activity  $\alpha \in (1, 2)$ , for which estimators of the drift, scaling and jump activity parameters from high-frequency observations of the process on a fixed time period have been proposed in previous work [BC23]. We first present a numerical scheme to simulate this process. Next, we describe the challenge presented by the non-symmetric stable Lévy process when computing its density and its derivatives. We finally implement the estimators and carry out simulations to show good estimation accuracy.

**Résumé.** Nous considérons un processus de Cox-Ingersoll-Ross stable ( $\alpha$ -stable CIR) dirigé par un processus de Lévy stable non symétrique d'indice d'activité des sauts  $\alpha \in (1, 2)$ , pour lequel des estimateurs des paramètres de tendance, d'échelle et d'activité des sauts à partir d'observations haute fréquence du processus sur une période de temps fixe ont été proposés dans des travaux antérieurs [BC23]. Nous présentons d'abord un schéma numérique pour simuler ce processus. Ensuite, nous décrivons la difficulté que représente le processus de Lévy stable non symétrique lors du calcul de sa densité et de ses dérivées. Enfin, nous implémentons les estimateurs et effectuons des simulations de Monte-Carlo pour montrer la bonne précision de l'estimation.

### INTRODUCTION

Many fields such as finance and neurosciences use models based on stochastic equations with jump. When modeling interest rates, this led to an extension of the classical Cox-Ingersoll-Ross process (CIR process) introduced in [CIR85] to the  $\alpha$ -stable CIR processes (see Jiao et al. [JMS17] and [JMSZ21]) described by

$$X_t = x_0 + at - b \int_0^t X_s ds + \sigma \int_0^t \sqrt{X_s} dB_s + \delta \int_0^t X_{s-}^{1/\alpha} dL_s^\alpha \quad t \geq 0$$

where  $(B_t)_{t \geq 0}$  is a standard Brownian motion and  $(L_t^\alpha)_{t \geq 0}$  a compensated non-symmetric spectrally positive  $\alpha$ -stable Lévy process with  $\alpha \in (1, 2)$ , both in dimension 1. We assume that the characteristic function of  $L_1^\alpha$  is given by

$$\mathbb{E}(e^{izL_1^\alpha}) = \exp\left(-|z|^\alpha \left(1 - i \tan \frac{\pi\alpha}{2} \operatorname{sgn}(z)\right)\right).$$

From Theorem 14.15 in Sato [Sat13], such a process is strictly self-similar ie  $L_t^\alpha \stackrel{\mathcal{L}}{=} t^{1/\alpha} L_1^\alpha$ . We denote by  $\varphi_\alpha$  the density of  $L_1^\alpha$ .

This paper follows previous work [BC23], which focused on the estimation of the drift parameters  $a$  and  $b$ , the scaling parameter  $\delta$  and the jump activity  $\alpha$  from high-frequency observations of the process on a fixed time

<sup>1</sup> elise.bayraktar@univ-eiffel.fr

period  $[0, T]$ . The estimation of the drift on a finite time interval is not feasible in the presence of a Brownian motion, so we considered a pure-jump  $\alpha$ -stable CIR process ( $\sigma = 0$  in the previous equation)

$$dX_t = (a_0 - b_0 X_t)dt + \delta_0 X_{t-}^{1/\alpha_0} dL_t^{\alpha_0}, \quad X_0 = x_0 > 0 \quad (1)$$

with  $a_0 > 0$ ,  $b_0 \in \mathbb{R}$ ,  $\delta_0 > 0$ . We know that (1) admits a pathwise unique strong solution and that this solution is positive, that is  $\mathbb{P}(\forall t \in [0, 1]; X_t > 0) = 1$  (see Fu and Li [FL10], Li and Mytnik [LM11], Jiao, Ma and Scotti [JMS17]).

The estimation proposed in [BC23] is based on estimating equations. We build an estimator by maximising a quasi-likelihood function, which we construct by approximating the conditional distribution of  $X_{t+h}$  given  $X_t$  by the stable distribution appropriately centered and rescaled (see Masuda [Mas19] and Clément and Gloter [CG20]). We also use the power variation method described by Todorov [Tod13] to build non-rate optimal estimators, then correct them using the one-step method. The one-step method was described by Masuda [Mas23] for the estimation of Ornstein-Uhlenbeck type processes. Brouste and Masuda [BM18] also used the one-step improvement for a stable Lévy process.

This paper aims to numerically implement the estimator proposed in [BC23] to illustrate its asymptotic properties. We notice that the previous study [BM18] was conducted for a symmetric Lévy process. In this paper, we are concerned with a non-symmetric Lévy process. Numerically, this makes the computation of the density and its derivatives harder, and the one-step correction more difficult to implement.

The paper is organised as follows. Section 1 presents the numerical scheme used to simulate the process that solves (1). Section 2 describes the challenge presented by the computation of the density of the non-symmetric stable Lévy process and its derivatives. Section 3 recalls the estimation method proposed in [BC23] as well as the asymptotic properties of estimators. Next, we describe in this section how to build the estimators in practice and we confirm numerically the theoretical convergences.

## 1. SIMULATING THE PROCESS

### 1.1. Numerical scheme

We want to generate the process  $(X_t)_{t \in [0, 1]}$  that solves equation (1) by using a discretisation scheme. We know that the solution  $X$  is positive with the choice of parameters  $a_0 > 0$  and  $\delta_0 > 0$ , we therefore want a scheme that preserves this positivity. We use the discretisation scheme proposed by Li and Taguchi [LT19]. For technical reasons, this scheme uses a truncation and considers a bounded jump coefficient in order to prove consistency. Denoting by  $X_t^H$  the solution of

$$dX_t^H = (a_0 - b_0 X_t^H)dt + \delta_0 h(X_{t-}^H) dL_t^{\alpha_0}, \quad X_0^H = x_0 > 0$$

where  $h(x) = \min\{|x|^{1/\alpha_0}, H\}$  for some arbitrarily large constant  $H > 1$ , they consider the following positivity preserving semi-explicit scheme :  $X_0^{H,n} = x_0$  and for  $i \geq 0$

$$X_{\frac{i+1}{n}}^{H,n} = \frac{|X_{\frac{i}{n}}^{H,n} + \frac{a_0}{n} + \delta_0 h(X_{\frac{i}{n}}^{H,n}) \Delta_i^n L^{\alpha_0}|}{(1 + \frac{b_0}{n})}. \quad (2)$$

Assuming  $\alpha_0 \in (\sqrt{2}, 2)$ , they get in Corollary 2.9 a strong rate of convergence. For any  $p \in (0, \alpha_0^2 - 2)$ , setting  $H = Kn^l$  for  $l = \frac{(2/\alpha_0 - 1)/(4\alpha_0)}{1 + p(1 - \alpha_0/2)}$ , there exists  $C_{T,p} > 0$  such that

$$\sup_{t \leq T} \mathbb{E}(|X_t - X_t^{n,l}|) \leq C_{T,p} n^{-L} \quad (3)$$

where  $L = (2/\alpha_0 - 1)/(4\alpha_0) - l$  and  $C_{T,p}$  converges to infinity as  $p$  increases to  $\alpha_0^2 - 2$ . In practice,  $H = Kn^l \rightarrow \infty$  as  $n \rightarrow \infty$  and the smallest value of  $n$  used in the simulations will be 128000. Hence we use  $H = +\infty$  which

corresponds to no truncation or  $h(x) = |x|^{1/\alpha_0}$ . We numerically confirm, taking  $x_0 = 1$  and  $H = 10n^l$ , that even for extreme values such as  $\alpha_0 = 1.99$  and  $n = 128000$  that we never reach the truncation when simulating 1000 trajectories.

## 1.2. Generation of a $\alpha$ -stable random variable

The previous discretisation scheme relies on simulating the independent increments of the Lévy process  $\Delta_i^n L^{\alpha_0} = L_{\frac{i}{n}}^{\alpha_0} - L_{\frac{i-1}{n}}^{\alpha_0} \stackrel{\mathcal{L}}{=} L_{1/n}^{\alpha_0}$ . Using the self-similarity property of  $(L_t^{\alpha_0})_{t \in [0,1]}$ , we know that  $\Delta_i^n L^{\alpha_0} \stackrel{\mathcal{L}}{=} n^{-1/\alpha_0} L_1^{\alpha_0}$ . Therefore, we only need to simulate independent copies of  $L_1^{\alpha_0}$ . We use the method presented in Weron [WW95] to generate  $L_1^{\alpha,\beta}$  a  $\alpha$ -stable random variable,  $\alpha \in (0, 2)$  and  $\alpha \neq 1$ , of skewness parameter  $\beta \in [-1, 1]$ , with characteristic function

$$\Phi^{\alpha,\beta}(z) = \mathbb{E} \left( e^{izL_1^{\alpha,\beta}} \right) = \exp \left( -|z|^\alpha \left( 1 - i\beta \tan \left( \frac{\pi\alpha}{2} \right) \operatorname{sgn}(z) \right) \right). \quad (4)$$

This method is based on the simulation of  $V$  a uniform random variable on  $(-\frac{\pi}{2}, \frac{\pi}{2})$  and an independent exponential random variable  $W$  with mean 1. Using these variables, we get a  $\alpha$ -stable random variable  $L_1^{\alpha,\beta}$  by

$$L_1^{\alpha,\beta} = S_{\alpha,\beta} \times \frac{\sin(\alpha(V + B_{\alpha,\beta}))}{(\cos(V))^{1/\alpha}} \times \left( \frac{\cos(V - \alpha(V + B_{\alpha,\beta}))}{W} \right)^{(1-\alpha)/\alpha}, \quad (5)$$

where

$$B_{\alpha,\beta} = \frac{\arctan(\beta \tan \frac{\alpha\pi}{2})}{\alpha}, \quad S_{\alpha,\beta} = \left( 1 + \beta^2 \tan^2 \frac{\alpha\pi}{2} \right)^{1/(2\alpha)}. \quad (6)$$

In this paper, we will consider  $\alpha$ -stable variables with  $\beta = 1$ ,  $\alpha \in (1, 2)$ .

Using independent uniform and exponential random variables, we are now able to simulate independent copies of  $L_1^\alpha = L_1^{\alpha,1}$ . We can now simulate the process  $(X_t)_{t \in [0,1]}$  that solves (1) using the numerical scheme (2) with  $H = +\infty$ . For the rest of the simulations, we will consider high-frequency observations  $(X_{\frac{i}{n}})_{1 \leq i \leq n}$  on  $[0, 1]$ . To have a more accurate simulation of our process, we use the numerical scheme with step  $\frac{1}{1000} \frac{1}{n}$ . We show in Figure 1 some simulated trajectories for different parameter values with  $\frac{1}{n} = \frac{1}{500}$ .

## 2. COMPUTING THE DENSITY OF A STRICTLY $\alpha$ -STABLE PROCESS

To estimate the parameters, we use a quasi-likelihood method based on the density  $\varphi_\alpha$  of a strictly  $\alpha$ -stable random variable  $L_1^\alpha = L_1^{\alpha,1}$ . We now explain how to compute this density and its derivatives efficiently.

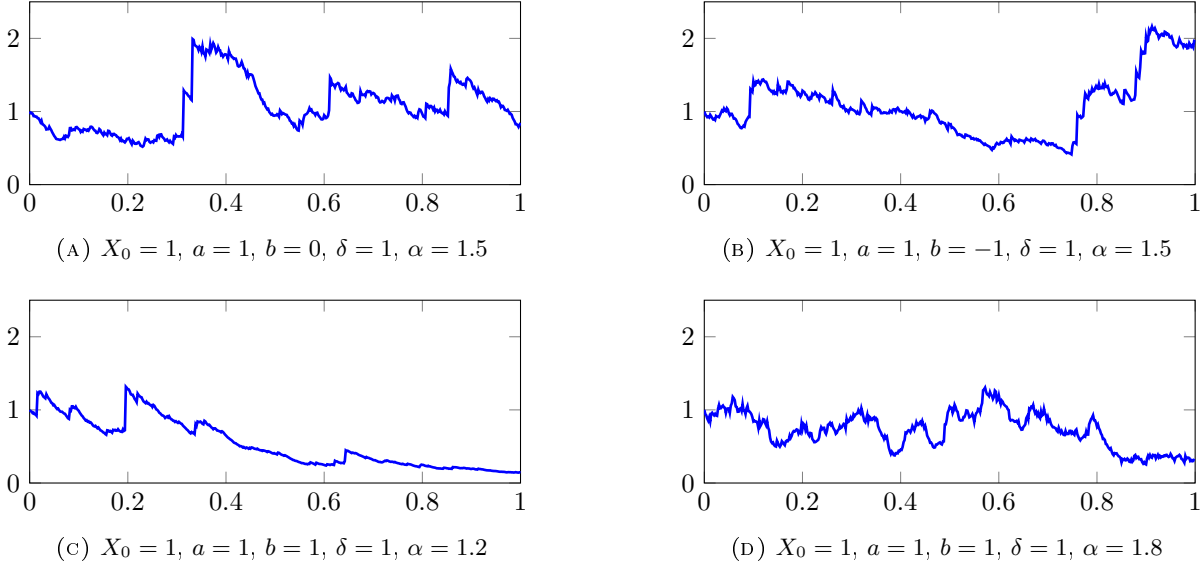
### 2.1. Density of a strictly $\alpha$ -stable process

The characteristic function of  $L_1^\alpha$  has the following expression

$$\Phi^{\alpha,1}(z) = \mathbb{E} \left( e^{izL_1^\alpha} \right) = \exp \left( -|z|^\alpha \left( 1 - i \tan \left( \frac{\pi\alpha}{2} \right) \operatorname{sgn}(z) \right) \right). \quad (7)$$

We could compute the density  $\varphi_\alpha$  using the Fourier inversion of the characteristic function, but this would result in an integral on  $\mathbb{R}$ . We instead use the expression presented in Nolan [Nol97], with an integral on a bounded interval which allows for an easy numerical computation of this density. In [Nol97], Nolan gives a computation of the density of a  $\alpha$ -stable random variable  $Y$  with characteristic function

$$\begin{aligned} \mathbb{E} \left( e^{izY} \right) &= \exp \left( -|z|^\alpha \left( 1 + i\beta \tan \left( \frac{\pi\alpha}{2} \right) \operatorname{sgn}(z) (|z|^{1-\alpha} - 1) \right) \right) \\ &= \mathbb{E} \left( e^{iz(L_1^\alpha - \beta \tan(\frac{\pi\alpha}{2}))} \right). \end{aligned} \quad (8)$$


 FIGURE 1. Simulation of trajectories of the  $\alpha$ -CIR process

For such a random variable, and denoting by  $f$  its density function, the following representation holds:

$$f(x, \alpha, \beta) = \begin{cases} \frac{\alpha(x-\xi)^{1/(\alpha-1)}}{\pi|\alpha-1|} \int_{-B_{\alpha,\beta}}^{\pi/2} V(\theta, \alpha, \beta) \exp(-(x-\xi)^{\alpha/(\alpha-1)} V(\theta, \alpha, \beta)) d\theta & x > \xi \\ \frac{\Gamma(1+1/\alpha) \cos(B_{\alpha,\beta})}{\pi(1+\xi^2)^{1/(2\alpha)}} & x = \xi \\ f(-x, \alpha, -\beta) & x < \xi \end{cases} \quad (9)$$

where  $\xi = -\beta \tan \frac{\pi\alpha}{2}$ ,  $\Gamma(a) = \int_0^\infty x^{a-1} e^{-x} dx$ ,  $B_{\alpha,\beta}$  is defined in (6) and

$$V(\theta, \alpha, \beta) = (\cos(\alpha B_{\alpha,\beta}))^{1/(\alpha-1)} \left( \frac{\cos \theta}{\sin(\alpha(\theta + B_{\alpha,\beta}))} \right)^{\alpha/(\alpha-1)} \frac{\cos(\alpha B_{\alpha,\beta} + (\alpha-1)\theta)}{\cos \theta}.$$

As highlighted by the characteristic functions (8) and (7), we have  $Y = L_1^\alpha + \xi$ . Hence, we get  $\varphi_\alpha$  the density of  $L_1^\alpha$  by

$$\varphi_\alpha(x) = f(x + \xi, \alpha, 1), \quad \forall x \in \mathbb{R}. \quad (10)$$

This density is available in the Python package Scipy [VGO<sup>+</sup>20] with the `scipy.stats.levy_stable` function, or in the R package *RStableDist* [WMctm16]. Figure 2 gives the graph of the density for different values of  $\alpha$ .

We can also check that this distribution is coherent with simulations done in Section 1.2. We generate independent copies of  $L_1^\alpha$  according to equation (5) and compare the obtained distribution to the expected density as computed in (10). Figure 3 compares the density to the histogram of the obtained density when simulating  $n_{copies} = 100000$  independent copies of  $L_1^\alpha$ .

For the rest of the simulations, we will use the scipy density because it has been optimised and makes the computations faster, but the explicit expression of the density is useful later when trying to compute the derivatives.

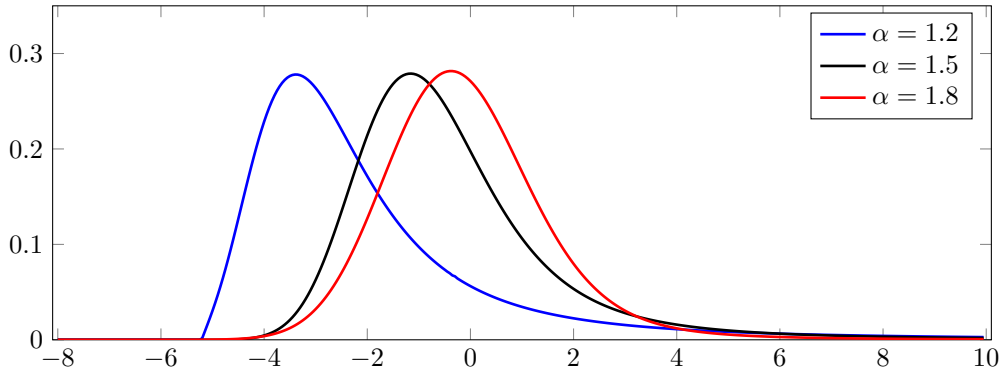


FIGURE 2. Graphs of the  $\alpha$ -stable density  $\varphi_\alpha$  ( $\beta=1$ ) for different values of  $\alpha$

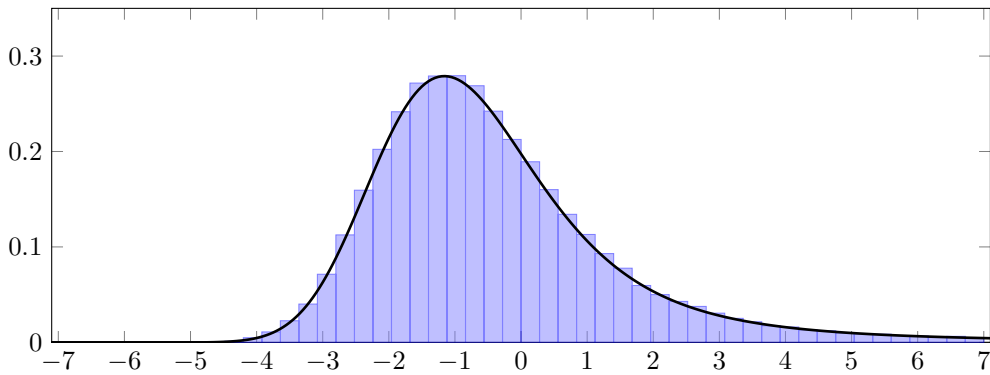


FIGURE 3. Distribution of simulated  $\alpha$ -stable random variable ( $\alpha = 1.5$ ,  $\beta = 1$ ,  $n_{copies} = 100000$  variables) and comparison with the expected density  $\varphi_\alpha$

## 2.2. Derivatives of the density

The correction that we will apply to our first-step estimator uses the density  $\varphi_\alpha$  and its derivatives. For symmetric  $\alpha$ -stable distributions, a method for efficient evaluation of the derivatives of the density has been studied in Matsui and Tamekura [MT06]. Similarly to what is done for the symmetric process, we use the derivative of expression (9) to get the derivative with respect to  $x$  of the density. For  $x > \xi$ , we have (where  $f' = \partial_x f$ )

$$f'(x, \alpha, \beta) = \frac{\alpha x^{1/(\alpha-1)}}{\pi|\alpha-1|} \left( \frac{1}{x(\alpha-1)} \int_{-B_{\alpha,\beta}}^{\pi/2} V(\theta, \alpha, \beta) \exp(-x^{\alpha/(\alpha-1)} V(\theta, \alpha, \beta)) d\theta \right. \\ \left. - \frac{\alpha}{\alpha-1} x^{1/(\alpha-1)} \int_{-B_{\alpha,\beta}}^{\pi/2} V(\theta, \alpha, \beta)^2 \exp(-x^{\alpha/(\alpha-1)} V(\theta, \alpha, \beta)) d\theta \right),$$

and for  $x < \xi$

$$f'(x, \alpha, \beta) = -f'(-x, \alpha, -\beta).$$

We conclude using that

$$\varphi'_\alpha(x) = f'(x + \xi, \alpha, 1). \tag{11}$$

We confirm this expression of the derivative by comparing it to a two-point estimate and see that it agrees. In Figure 4, we give the graph of the derivative of the density for two values of  $\alpha$ .

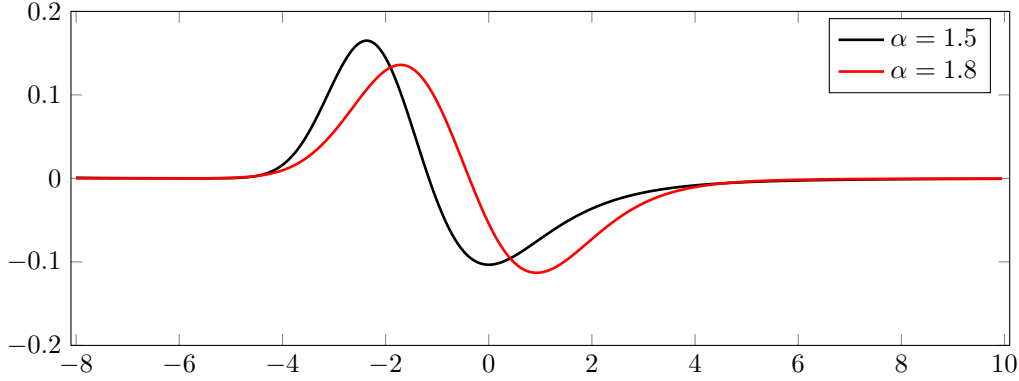


FIGURE 4. Graph of  $\varphi'_\alpha$  for  $\alpha_0 = 1.5$  and  $\alpha_0 = 1.8$

We now want to compute  $\partial_\alpha \varphi_\alpha$ . Contrary to the symmetric case presented in Matsui and Tamekura [MT06], the bound of the integral given by the  $B_{\alpha,\beta}$  parameter defined in (6) depends on  $\alpha$ . Hence for  $x > \xi$

$$\begin{aligned} \partial_\alpha f(x, \alpha, \beta) &= \partial_\alpha \left( \frac{\alpha(x - \xi)^{1/(\alpha-1)}}{\pi|\alpha-1|} \right) \int_{-B_{\alpha,\beta}}^{\pi/2} V(\theta, \alpha, \beta) \exp(-(x - \xi)^{\alpha/(\alpha-1)} V(\theta, \alpha, \beta)) d\theta \\ &+ \frac{\alpha(x - \xi)^{1/(\alpha-1)}}{\pi|\alpha-1|} \int_{-B_{\alpha,\beta}}^{\pi/2} \partial_\alpha \left[ V(\theta, \alpha, \beta) \exp(-(x - \xi)^{\alpha/(\alpha-1)} V(\theta, \alpha, \beta)) \right] d\theta \\ &+ \frac{\alpha(x - \xi)^{1/(\alpha-1)}}{\pi|\alpha-1|} \partial_\alpha(B_{\alpha,\beta}) V(-B_{\alpha,\beta}, \alpha, \beta) \exp(-(x - \xi)^{\alpha/(\alpha-1)} V(-B_{\alpha,\beta}, \alpha, \beta)). \end{aligned}$$

We see that this expression is costly to compute. In practice, it leads to unstable results. We therefore choose a two-point estimate

$$\partial_\alpha \varphi_\alpha(x) \approx \frac{\varphi_{\alpha+h}(x) - \varphi_{\alpha-h}(x)}{2h}.$$

### 3. MONTE-CARLO ESTIMATORS

#### 3.1. Estimation method

We assume that observations  $(X_{\frac{i}{n}})_{1 \leq i \leq n}$  are given by the stochastic equation (1) for the true parameter value  $\theta_0 = (a_0, b_0, \delta_0, \alpha_0)$ . This paper is a follow-up to the previous article [BC23] in which we propose estimators of the parameter  $\theta = (a, b, \delta, \alpha)$  and study their asymptotic properties. Following [BC23] we propose a first-step estimator, which is fairly easy to compute but is not rate optimal. This estimator will then be corrected to reach an efficient estimator.

We first estimate the jump activity coefficient  $\alpha_0$  by the power variation method described in Todorov [Tod13]

$$\tilde{\alpha}_n = \frac{\ln 2}{2 \ln(V_n^2(1/2, X)/V_n^1(1/2, X))} \mathbb{1}_{V_n^1(1/2, X) \neq V_n^2(1/2, X)} \quad (12)$$

where

$$V_n^1(p, X) = \sum_{i=2}^n |\Delta_i^n X - \Delta_{i-1}^n X|^p \quad \text{with } \Delta_i^n X = X_{\frac{i}{n}} - X_{\frac{i-1}{n}},$$

$$V_n^2(p, X) = \sum_{i=4}^n |\Delta_i^n X - \Delta_{i-1}^n X + \Delta_{i-2}^n X - \Delta_{i-3}^n X|^p.$$

This estimator is easy and quick to compute numerically.

The scaling parameter  $\delta_0$  is next estimated, using again a power-variation method

$$\tilde{\delta}_n = \left( \frac{1}{m_{1/2}(\tilde{\alpha}_n)} \frac{1}{n} \sum_{i=2}^n n^{1/2\tilde{\alpha}_n} \frac{|X_{\frac{i}{n}} - 2X_{\frac{i-1}{n}} + X_{\frac{i-2}{n}}|^{1/2}}{X_{\frac{i-2}{n}}^{1/2\tilde{\alpha}_n}} \right)^2 \quad (13)$$

with  $m_{1/2}(\alpha) = \mathbb{E}(|2^{1/\alpha} S_1^\alpha|^{1/2})$  where  $S_1^\alpha$  has a symmetric  $\alpha$ -stable distribution. From Masuda [Mas09], we have  $\forall q \in (-1, \alpha)$ ,  $\mathbb{E}|S_1^\alpha|^q = \frac{2^q \Gamma(\frac{q+1}{2}) \Gamma(1-\frac{q}{\alpha})}{\sqrt{\pi} \Gamma(1-\frac{q}{2})}$ . Hence  $m_{1/2}(\tilde{\alpha}_n)$  has an explicit expression and is easy to compute, and so is  $\tilde{\delta}_n$ .

To estimate the drift parameters  $(a, b)$ , we consider the quasi-likelihood function given by (recalling that  $\theta = (a, b, \delta, \alpha)$ )

$$L_n(\theta) = \sum_{i=1}^n \ln \left( \frac{n^{1/\alpha}}{\delta X_{\frac{i-1}{n}}^{1/\alpha}} \varphi_\alpha(z_i^n(\theta)) \right) \quad \text{with } z_i^n(\theta) = n^{1/\alpha} \frac{X_{\frac{i}{n}} - X_{\frac{i-1}{n}} - \frac{a}{n} + \frac{b}{n} X_{\frac{i-1}{n}}}{\delta X_{\frac{i-1}{n}}^{1/\alpha}}. \quad (14)$$

When  $\delta_0$  and  $\alpha_0$  are known, we maximise the quasi-likelihood function  $(a, b) \rightarrow L_n(a, b, \delta_0, \alpha_0)$  to build the estimators of the drift  $(\hat{a}_n, \hat{b}_n)$ . Similarly, when  $\alpha_0$  and  $\delta_0$  are estimated by  $\tilde{\alpha}_n$  and  $\tilde{\delta}_n$ , we maximise  $(a, b) \rightarrow L_n(a, b, \tilde{\delta}_n, \tilde{\alpha}_n)$  and we denote by  $(\tilde{a}_n, \tilde{b}_n)$  the resulting estimators.

We introduce the notations  $h_\alpha(x) = \frac{\varphi'_\alpha}{\varphi_\alpha}(x)$ ,  $k_\alpha(x) = 1 + xh_\alpha(x)$ ,  $f_\alpha(x) = \frac{\partial_\alpha \varphi_\alpha}{\varphi_\alpha}(x)$  and

$$I^{11}(\theta) = \begin{pmatrix} \frac{1}{\delta^2} \int_0^1 \frac{1}{X_s^{2/\alpha}} ds \mathbb{E}(h_\alpha^2(L_1)) & \frac{-1}{\delta^2} \int_0^1 \frac{X_s}{X_s^{2/\alpha}} ds \mathbb{E}(h_\alpha^2(L_1)) \\ \frac{-1}{\delta^2} \int_0^1 \frac{X_s}{X_s^{2/\alpha}} ds \mathbb{E}(h_\alpha^2(L_1)) & \frac{1}{\delta^2} \int_0^1 \frac{X_s^2}{X_s^{2/\alpha}} ds \mathbb{E}(h_\alpha^2(L_1)) \end{pmatrix}. \quad (15)$$

We summarise in the next result the asymptotic properties of these estimators. These convergences are obtained for the stable convergence in law which is stronger than the usual convergence in law and appropriate to our statistical problem. This convergence is denoted by  $\xrightarrow{\mathcal{L}-s}$  and we refer to Jacod and Protter [JP12] for the definition and properties of the stable convergence in law.

**Theorem 3.1.** (i)  $\tilde{\alpha}_n$  given by (12) converges in probability to  $\alpha_0$  and  $\sqrt{n}(\tilde{\alpha}_n - \alpha_0)$  stably converges in law.  
(ii)  $\tilde{\delta}_n$  given by (13) converges in probability to  $\delta_0$  and  $\frac{\sqrt{n}}{\ln(n)}(\tilde{\delta}_n - \delta_0)$  is tight.  
(iii) For  $\alpha_0$  and  $\delta_0$  known, we have the stable convergence in law

$$n^{1/\alpha_0 - 1/2} \begin{pmatrix} \hat{a}_n - a_0 \\ \hat{b}_n - b_0 \end{pmatrix} \xrightarrow[n \rightarrow \infty]{\mathcal{L}-s} I^{11}(\theta_0)^{-1/2} \mathcal{N} \quad (16)$$

where  $\mathcal{N}$  is a standard Gaussian variable independent of  $I^{11}(\theta_0)$ .

(iv) For  $\tilde{\alpha}_n$  and  $\tilde{\delta}_n$  estimating  $\alpha_0$  and  $\delta_0$ ,  $\frac{n^{1/\alpha_0-1/2}}{\ln(n)^2} \begin{pmatrix} \tilde{\alpha}_n - a_0 \\ \tilde{\delta}_n - b_0 \end{pmatrix}$  is tight.

(i) is proven in Todorov [Tod13]. (ii) is proven in Theorem 4.3 of [BC23]. (iii) and (iv) are proven in Theorem 4.2 of [BC23].

We compute a preliminary estimator by successively estimating  $\tilde{\alpha}_n$  from (12) and  $\tilde{\delta}_n$  from (13). Then, we estimate the drift parameters  $(a, b)$  by maximising the quasi-likelihood function restricted to the drift  $(a, b) \rightarrow L_n(a, b, \tilde{\delta}_n, \tilde{\alpha}_n)$  with  $L_n$  defined in (14) and we denote by  $(\tilde{a}_n, \tilde{b}_n)$  the resulting estimators. We obtain a preliminary estimator  $\hat{\theta}_{0,n} = (\tilde{a}_n, \tilde{b}_n, \tilde{\delta}_n, \tilde{\alpha}_n)$ . For Theorem 3.1 this estimator is consistent but not rate optimal as we only prove the tightness of  $\ln(n)^{-2} u_n^{-1}(\hat{\theta}_{0,n} - \theta_0)$ , where

$$u_n^{-1} = \begin{pmatrix} n^{1/\alpha_0-1/2} \text{Id}_2 & 0 \\ 0 & \sqrt{n} \begin{pmatrix} \frac{1}{\delta_0} & \frac{\ln(n)}{\alpha_0^2} \\ 0 & 1 \end{pmatrix} \end{pmatrix}, \quad \text{Id}_2 = \begin{pmatrix} 1 & 0 \\ 0 & 1 \end{pmatrix}. \quad (17)$$

We correct this non-efficient preliminary estimator  $\hat{\theta}_{0,n}$  with a one-step procedure :

$$\hat{\theta}_{1,n} = \hat{\theta}_{0,n} - J_n(\hat{\theta}_{0,n})^{-1} G_n(\hat{\theta}_{0,n}), \quad (18)$$

where  $G_n = -\nabla_{\theta} \ln L_n(\theta)$  and  $J_n = \nabla_{\theta} G_n$ . We define

$$I(\theta) = \begin{pmatrix} I^{11}(\theta) & (I^{21}(\theta))^T \\ I^{21}(\theta) & I^{22}(\theta) \end{pmatrix} \quad (19)$$

where  $I^{11}(\theta)$  is defined in (15),  $(I^{21}(\theta))^T$  denotes the transpose of  $I^{21}(\theta)$  and

$$I^{21}(\theta) = \begin{pmatrix} \frac{1}{\delta} \int_0^1 \frac{ds}{X_s^{1/\alpha}} \mathbb{E}(h_{\alpha} k_{\alpha}(L_1^{\alpha})) & -\frac{1}{\delta} \int_0^1 \frac{X_s}{X_s^{1/\alpha}} ds \mathbb{E}(h_{\alpha} k_{\alpha}(L_1^{\alpha})) \\ I_{21}^{21}(\theta) & I_{21}^{22}(\theta) \end{pmatrix}, \quad I^{22}(\theta) = \begin{pmatrix} \mathbb{E}(k_{\alpha}^2(L_1^{\alpha})) & I_{21}^{22}(\theta) \\ I_{21}^{22}(\theta) & I_{22}^{22}(\theta) \end{pmatrix}$$

where

$$\begin{aligned} I_{21}^{21}(\theta) &= -\frac{1}{\delta \alpha^2} \int_0^1 \frac{\ln(X_s)}{X_s^{1/\alpha}} ds \mathbb{E}(h_{\alpha} k_{\alpha}(L_1^{\alpha})) - \frac{1}{\delta} \int_0^1 \frac{ds}{X_s^{1/\alpha}} \mathbb{E}(f_{\alpha} h_{\alpha}(L_1^{\alpha})) \\ I_{22}^{21}(\theta) &= \frac{1}{\delta \alpha^2} \int_0^1 \frac{\ln(X_s) X_s}{X_s^{1/\alpha}} ds \mathbb{E}(h_{\alpha} k_{\alpha}(L_1^{\alpha})) + \frac{1}{\delta} \int_0^1 \frac{X_s}{X_s^{1/\alpha}} ds \mathbb{E}(f_{\alpha} h_{\alpha}(L_1^{\alpha})) \\ I_{21}^{22}(\theta) &= -\frac{1}{\alpha^2} \int_0^1 \ln(X_s) ds \mathbb{E}(k_{\alpha}^2(L_1^{\alpha})) - \mathbb{E}(f_{\alpha} k_{\alpha}(L_1^{\alpha})) \\ I_{22}^{22}(\theta) &= \frac{1}{\alpha^4} \int_0^1 \ln(X_s)^2 ds \mathbb{E}(k_{\alpha}^2(L_1^{\alpha})) + \frac{2}{\alpha^2} \int_0^1 \ln(X_s) ds \mathbb{E}(f_{\alpha} k_{\alpha}(L_1^{\alpha})) + \mathbb{E}(f_{\alpha}^2(L_1^{\alpha})). \end{aligned}$$

**Corollary 3.2.** *We have the stable convergence in law, with  $I(\theta_0)$  defined in (19)*

$$u_n^{-1}(\hat{\theta}_{1,n} - \theta_0) \xrightarrow[n \rightarrow \infty]{\mathcal{L}-s} I(\theta_0)^{-1/2} \mathcal{N}.$$

This was proved in Corollary 4.1 of [BC23].

### 3.2. Simulation results for the first-step estimator

#### 3.2.1. Estimation of $\alpha$

In Table 1, we present results of numerical simulations conducted with the true value of the parameter  $\alpha_0 = 1.3$ . We let the number of data points  $n$  range in the set  $\{128, 256, 512, 1024, 2048, 4096\}$ . The process  $(X_t)$  is simulated according to the scheme (2) with step  $(1000n)^{-1}$ . We show a Monte-Carlo evaluation, based on  $n_{MC} = 1000$  replications, for the mean and standard deviation of the estimator  $\tilde{\alpha}_n$  given in (12).

n	Mean of $\tilde{\alpha}_n$	Standard deviation of $\tilde{\alpha}_n$
128	1.473	$3.65 * 10^{-1}$
256	1.396	$1.98 * 10^{-1}$
512	1.351	$1.27 * 10^{-1}$
1024	1.333	$8.88 * 10^{-2}$
2048	1.319	$6.25 * 10^{-2}$
4096	1.310	$4.65 * 10^{-2}$

TABLE 1. Mean and standard deviation of  $\tilde{\alpha}_n$  with 1000 replications

#### 3.2.2. Estimation of $\delta$

In Tables 2-3, we present results of numerical simulations for the estimator  $\tilde{\delta}_n$  given in (13) conducted with the true value of the parameter  $\delta_0 = 1$ , respectively for  $\alpha_0 = 1.3$  known and for  $\alpha_0$  estimated by  $\tilde{\alpha}_n$  as described in 3.2.1. We again let  $n$  range in the set  $\{128, 256, 512, 1024, 2048, 4096\}$  and simulate  $(X_t)$  using (2) with step  $(1000n)^{-1}$ . We give an estimation by Monte-Carlo of the mean of the estimators together with their standard deviations. In these Monte-Carlo experiments, we used  $n_{MC} = 1000$  replications. As expected,  $\tilde{\delta}_n$  converges to  $\delta_0$  both when  $\alpha_0$  is known and when it is estimated, but the convergence is slower when  $\alpha_0$  is unknown and has to be estimated. This corresponds to the loss of rate  $\ln(n)$  that happens when estimating  $\delta$  and  $\alpha$  simultaneously.

n	Mean of $\tilde{\delta}_n$	Std of $\tilde{\delta}_n$
128	0.944	$2.10 * 10^{-1}$
256	0.967	$1.41 * 10^{-1}$
512	0.983	$1.07 * 10^{-1}$
1024	0.988	$7.60 * 10^{-2}$
2048	0.994	$5.44 * 10^{-2}$
4096	0.998	$3.92 * 10^{-2}$

TABLE 2. Mean and standard deviation of  $\tilde{\delta}_n$  for  $\alpha_0 = 1.3$  known with 1000 replications

n	Mean of $\tilde{\delta}_n$	Std of $\tilde{\delta}_n$
128	0.859	$4.93 * 10^{-1}$
256	0.899	$3.79 * 10^{-1}$
512	0.932	$3.52 * 10^{-1}$
1024	0.941	$2.89 * 10^{-1}$
2048	0.959	$2.31 * 10^{-1}$
4096	0.978	$1.94 * 10^{-1}$

TABLE 3. Mean and standard deviation of  $\tilde{\delta}_n$  for  $\tilde{\alpha}_n$  estimating  $\alpha_0$  with 1000 replications

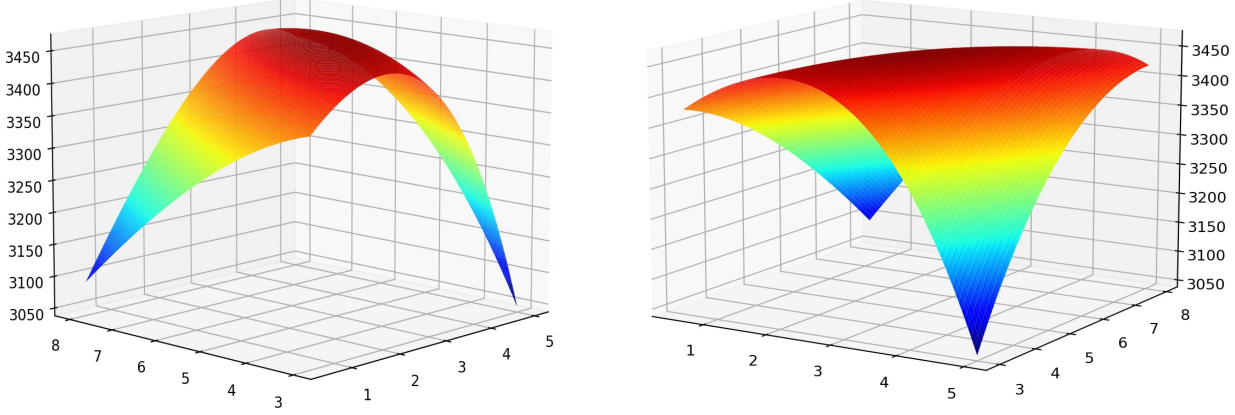


FIGURE 5. Views of the quasi-likelihood

### 3.2.3. Estimation of the drift for $\delta_0$ and $\alpha_0$ known

To have an idea of what the quasi-likelihood function (14) looks like, we simulate one sample path of observations  $(X_{\frac{i}{n}})_{i=0,\dots,n}$  with  $n = 1000$ ,  $a_0 = 3$ ,  $b_0 = 5$ ,  $\delta_0 = 1$  and  $\alpha_0 = 1.3$ , and we plot in Figure 5 the graph of

$$\begin{aligned} [0.5, 5] \times [3, 8] &\rightarrow \mathbb{R} \\ (a, b) &\rightarrow L_n(a, b, \delta_0, \alpha_0). \end{aligned}$$

This quasi-likelihood function is concave. We see that the maximum in  $(a, b)$  is reached near the true value  $(a_0, b_0)$ . Maximising with respect to the two parameters using the Python Scipy package, we get  $(\hat{a}_n, \hat{b}_n) = (3.047, 5.068)$ . We can see that there is an area where the quasi-likelihood doesn't vary much. This can lead to difficulties when maximising it, especially later for estimated values of  $\delta$  and  $\alpha$ .

The maximisation of  $L_n$  is conducted using quasi-Newton methods implemented in Python Scipy package. It necessitates to compute numerically the values of the quasi-likelihood function as detailed in Section 2, and thus involves the numerous evaluations of  $(\varphi_\alpha(z_i^n(\theta)))_{i=1,\dots,n}$ . To make the estimation faster, these computations can be parallelised using the Python package Joblib.

In order to check the convergence (16), in which the asymptotic law is conditionally Gaussian, we will check that for  $\Sigma = I^{11}(\theta_0)^{-1}$

$$n^{1/\alpha_0-1/2}(\hat{a}_n - a_0) \xrightarrow[n \rightarrow \infty]{\mathcal{L}\text{-}s} \sqrt{\Sigma_{11}}\mathcal{N} \quad \text{and} \quad n^{1/\alpha_0-1/2}(\hat{b}_n - b_0) \xrightarrow[n \rightarrow \infty]{\mathcal{L}\text{-}s} \sqrt{\Sigma_{22}}\mathcal{N}.$$

We estimate  $\Sigma$  by  $\Sigma_n = I_n^{11}(\theta_0)^{-1}$  with

$$I_n^{11}(\theta_0) = \frac{1}{n} \sum_{i=1}^n \begin{pmatrix} \frac{1}{\delta_0^2} \frac{1}{X_{\frac{i-1}{n}}^{2/\alpha_0}} \mathbb{E}(h_{\alpha_0}^2(L_1^{\alpha_0})) & \frac{-1}{\delta_0^2} \frac{X_{\frac{i-1}{n}}}{X_{\frac{i-1}{n}}^{2/\alpha_0}} \mathbb{E}(h_{\alpha_0}^2(L_1^{\alpha_0})) \\ \frac{-1}{\delta_0^2} \frac{X_{\frac{i-1}{n}}}{X_{\frac{i-1}{n}}^{2/\alpha_0}} \mathbb{E}(h_{\alpha_0}^2(L_1^{\alpha_0})) & \frac{1}{\delta_0^2} \frac{X_{\frac{i-1}{n}}^2}{X_{\frac{i-1}{n}}^{2/\alpha_0}} \mathbb{E}(h_{\alpha_0}^2(L_1^{\alpha_0})) \end{pmatrix}$$

where  $\mathbb{E}(h_{\alpha_0}^2(L_1^{\alpha_0}))$  is calibrated once with a Monte-Carlo method with a very large  $n_{MC} = 100000$ . The proof of Theorem 3.1. in [BC23] shows that  $I_n^{11}(\theta_0)$  converges in probability to  $I^{11}(\theta_0) > 0$  which allows us to conclude

$$((\Sigma_n)_{11})^{-1/2} n^{1/\alpha_0-1/2}(\hat{a}_n - a_0) \xrightarrow[n \rightarrow \infty]{\mathcal{L}} \mathcal{N} \quad \text{and} \quad ((\Sigma_n)_{22})^{-1/2} n^{1/\alpha_0-1/2}(\hat{b}_n - b_0) \xrightarrow[n \rightarrow \infty]{\mathcal{L}} \mathcal{N}.$$

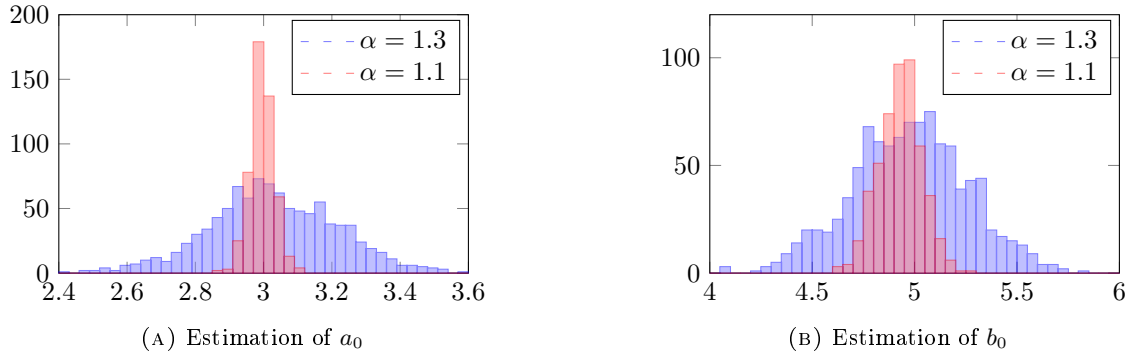


FIGURE 6. Impact of  $\alpha_0$  on the convergence of the drift  
( $a_0 = 3$ ,  $b_0 = 5$ ,  $\delta_0 = 1$ ,  $n=2048$ )

n	Mean of $\hat{a}_n$	Std of $\hat{a}_n$	Mean of $\hat{b}_n$	Std of $\hat{b}_n$
128	3.064	$4.25 * 10^{-1}$	4.633	$5.61 * 10^{-1}$
256	3.056	$3.53 * 10^{-1}$	4.779	$4.64 * 10^{-1}$
512	3.056	$2.86 * 10^{-1}$	4.895	$4.10 * 10^{-1}$
1024	3.038	$2.44 * 10^{-1}$	4.929	$3.24 * 10^{-1}$
2048	3.029	$2.08 * 10^{-1}$	4.976	$2.84 * 10^{-1}$
4096	3.024	$1.69 * 10^{-1}$	4.981	$2.37 * 10^{-1}$

TABLE 4. Mean and standard deviation of the drift estimators with  $\delta_0 = 1$  and  $\alpha_0 = 1.3$  known, with 1000 replications

From Table 4, we see that assuming  $\delta_0$  and  $\alpha_0$  known the joint estimation of drift parameters works well, but with a relatively slow rate of convergence  $n^{1/\alpha_0-1/2}$ . Hence this estimation works better for a value of  $\alpha_0$  closer to 1. This is also highlighted by Figure 6, where the convergence is a lot quicker for  $\alpha_0 = 1.1$  where  $n^{1/\alpha_0-1/2} \approx n^{0.41}$ , than for  $\alpha_0 = 1.3$  where  $n^{1/\alpha_0-1/2} \approx n^{0.27}$ .

In Table 5, we see that the asymptotic behaviour of the estimator is as predicted from the theoretical study, the rate of estimation for  $(\hat{a}_n, \hat{b}_n)$  is  $n^{1/\alpha_0-1/2}$  and the asymptotic rescaled standard deviations are very close to the theoretical one.

n	$((\Sigma_n)_{11})^{-1/2} n^{1/\alpha_0-1/2} (\hat{a}_n - a_0)$		$((\Sigma_n)_{22})^{-1/2} n^{1/\alpha_0-1/2} (\hat{b}_n - b_0)$	
	Mean	Std	Mean	Std
128	$7.86 * 10^{-2}$	0.954	$-6.54 * 10^{-1}$	0.946
256	$9.75 * 10^{-2}$	0.959	$-4.75 * 10^{-1}$	0.937
512	$1.52 * 10^{-1}$	0.983	$-2.75 * 10^{-1}$	0.982
1024	$1.25 * 10^{-1}$	0.985	$-2.32 * 10^{-1}$	0.946
2048	$1.34 * 10^{-1}$	0.964	$-1.04 * 10^{-1}$	0.998
4096	$1.20 * 10^{-2}$	0.972	$-9.34 * 10^{-2}$	0.988
Theoretical limit	0	1	0	1

TABLE 5. Mean and standard deviation of the rescaled errors

In Figure 7, we plot the distributions of the rescaled errors of estimation together with their Gaussian limits. We see that the empirical distributions fit very well the theoretical ones.

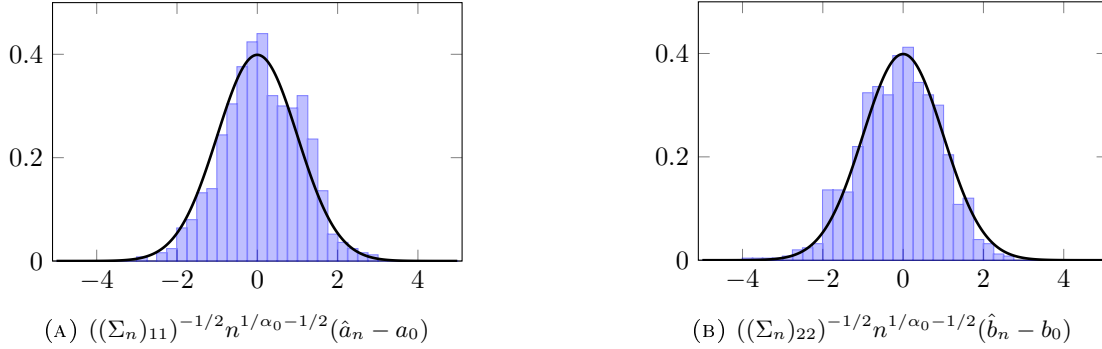


FIGURE 7. Distribution of the rescaled errors of estimation and comparison with  $\mathcal{N}(0, 1)$   
 $(a_0 = 3, b_0 = 5, \delta_0 = 1, \alpha_0 = 1.3, n = 2048)$

### 3.3. Simulation results for the one-step correction

In the following, we aim to show that the joint estimation of  $\theta = (a, \delta, \alpha)$  is feasible in practice, assuming  $b_0 = 5$  known, and that the one-step improvement leads to a rate-efficient estimator. The gradient and Hessian of the quasi-likelihood function  $G_n$  and  $J_n$  will be computed using finite differences, for reasons explained in Section 2.2. For this estimation, the theoretical variance is  $\bar{\Sigma} = \bar{I}(\theta_0)^{-1}$  with

$$\bar{I}(\theta_0) = \begin{pmatrix} \frac{1}{\delta_0^2} \int_0^1 \frac{1}{X_s^{2/\alpha_0}} ds \mathbb{E}(h_{\alpha_0}^2(L_1^{\alpha_0})) & \frac{1}{\delta_0} \int_0^1 \frac{ds}{X_s^{1/\alpha_0}} \mathbb{E}(h_{\alpha_0} k_{\alpha_0}(L_1^{\alpha_0})) & I_{21}^{21}(\theta) \\ \frac{1}{\delta_0} \int_0^1 \frac{ds}{X_s^{1/\alpha_0}} \mathbb{E}(h_{\alpha_0} k_{\alpha_0}(L_1^{\alpha_0})) & \mathbb{E}(k_{\alpha_0}^2(L_1^{\alpha_0})) & I_{21}^{22}(\theta) \\ I_{21}^{21}(\theta) & I_{21}^{22}(\theta) & I_{22}^{22}(\theta) \end{pmatrix}$$

the restriction of  $I(\theta_0)$  (defined in (19)) to the estimation of  $(a, \delta, \alpha)$ . We estimate  $\bar{\Sigma} = \bar{I}(\theta_0)^{-1}$  by  $\bar{\Sigma}_n = \bar{I}_n^{-1}$  where the integrals are estimated by Riemann sums, and the expectations are calibrated once with a Monte-Carlo method with a very large  $n_{MC} = 100000$ . For instance

$$(\bar{I}_n(\theta_0))_{11} = \frac{1}{\delta_0^2} \frac{1}{n} \sum_{i=1}^n \frac{1}{X_{\frac{i-1}{n}}^{2/\alpha_0}} \mathbb{E}(h_{\alpha_0}^2(L_1^{\alpha_0})).$$

We have proved in [BC23] that  $\bar{I}_n(\theta_0)$  converges in probability to  $\bar{I}(\theta_0) > 0$ . Hence from (19) we have the convergences in law

$$\begin{aligned} ((\bar{\Sigma}_n)_{11})^{-1/2} n^{1/\alpha_0 - 1/2} (\hat{a}_{1,n} - a_0) &\xrightarrow[n \rightarrow \infty]{\mathcal{L}-s} \mathcal{N}, \\ ((\bar{\Sigma}_n)_{33})^{-1/2} \frac{\sqrt{n}}{\ln(n)} \frac{\alpha_0^2}{\delta_0} (\hat{\delta}_{1,n} - \delta_0) &\xrightarrow[n \rightarrow \infty]{\mathcal{L}-s} \mathcal{N}, \\ ((\bar{\Sigma}_n)_{33})^{-1/2} \sqrt{n} (\hat{\alpha}_{1,n} - \alpha_0) &\xrightarrow[n \rightarrow \infty]{\mathcal{L}-s} \mathcal{N}. \end{aligned}$$

We consider larger values of  $n$  than we did previously, as smaller values such as  $n = 512$  lead to mixed results. We have once again simulated the process  $(X_t)$  using the scheme described in (2) with step  $(1000n)^{-1}$ . For these simulations, we chose  $a_0 = 3, b_0 = 5, \delta_0 = 1$  and  $\alpha_0 = 1.3$ . The following results are obtained with  $n_{MC} = 1000$  replications.

From Tables 6 and 7, we can check the impact of the one-step improvement. While the mean converges and the standard deviation decreases as  $n$  increases for both the preliminary and corrected estimators, we can

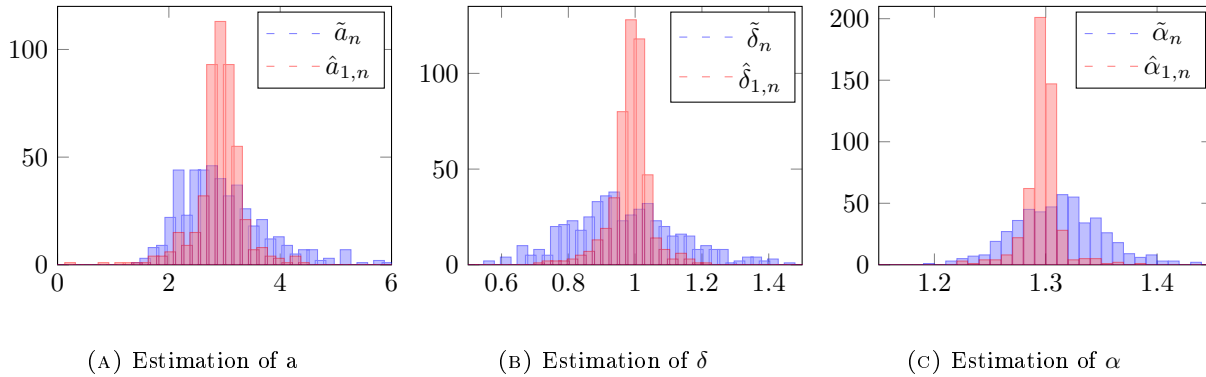


FIGURE 8. Distribution of estimation before and after one-step improvement  
 $(a_0 = 3, b_0 = 5, \delta_0 = 1, \alpha_0 = 1.3, n = 5000)$

see that the corrected estimators have much lower standard deviations. This significant improvement is also very clear in Figure 8. While both estimators are centered around the true value of the parameters, the lower variance of the one-step estimator leads to a more accurate estimation.

n	Mean of $\tilde{a}_n$	Mean of $\hat{a}_{1,n}$	Mean of $\tilde{\delta}_n$	Mean of $\hat{\delta}_{1,n}$	Mean of $\tilde{\alpha}_n$	Mean of $\hat{\alpha}_{1,n}$
2048	3.017	2.854	0.948	0.984	1.322	1.289
4096	3.011	2.913	0.962	0.989	1.314	1.294
8192	3.020	2.932	0.976	0.991	1.307	1.298

TABLE 6. Mean of the estimators before and after correction,  
with 1000 replications

n	Std of $\tilde{a}_n$	Std of $\hat{a}_{1,n}$	Std of $\tilde{\delta}_n$	Std of $\hat{\delta}_{1,n}$	Std of $\tilde{\alpha}_n$	Std of $\hat{\alpha}_{1,n}$
2048	1.15	0.875	$2.22 * 10^{-1}$	$1.19 * 10^{-1}$	$6.18 * 10^{-2}$	$4.43 * 10^{-2}$
4096	$7.99 * 10^{-1}$	$5.27 * 10^{-1}$	$1.87 * 10^{-1}$	$7.55 * 10^{-2}$	$4.67 * 10^{-2}$	$2.24 * 10^{-2}$
8192	$8.45 * 10^{-1}$	$4.37 * 10^{-1}$	$1.44 * 10^{-1}$	$5.07 * 10^{-2}$	$3.16 * 10^{-2}$	$1.21 * 10^{-2}$

TABLE 7. Standard deviation of the estimators before and after correction,  
with 1000 replications

In Figure 9, we plot the distributions of the rescaled errors of estimation of the one-step estimator, together with the standard Gaussian. Considering the number of approximations involved in the numerical computation of the one-step correction coming both from  $\varphi_\alpha$  and its derivatives, as detailed in Section 2, we see that the empirical distributions of the one-step estimator fit the theoretical ones.

**Remark 3.3.** When estimating  $\alpha$  in Section 3.2.1, we already had a rate of convergence  $\sqrt{n}$ , which is the same as the efficient rate. The improvement visible in Figure 8 comes from the better variance. This is also true for the estimation of  $\delta$ . On the other hand, the estimation of the drift gains in rate with this improvement.

**Remark 3.4.** We also know from Section 5.6 in [BC23] that, for some neighbourhood of  $\theta_0$   $V_n^{(n)}$ ,

$$\sup_{\theta \in V_n^{(n)}} \left| u_n^T J_n(\theta) u_n - I(\theta_0) \right| \rightarrow 0.$$

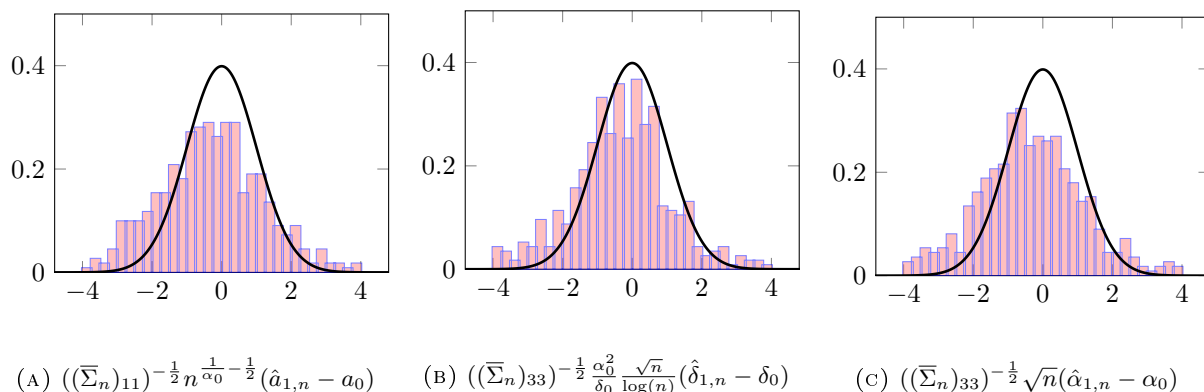


FIGURE 9. Distribution of the rescaled errors of estimation after the one-step improvement, and comparison with  $\mathcal{N}(0, 1)$   
 $(a_0 = 3, b_0 = 5, \delta_0 = 1, \alpha_0 = 1.3, n = 5000)$

So we could try using  $(u_n^T)^{-1} I(\hat{\theta}_{0,n}) u_n^{-1}$  instead of  $J_n(\hat{\theta}_{0,n})$  in our one-step procedure. However, numerical computations show similar results in both cases. Moreover, we would need to estimate  $I(\hat{\theta}_{0,n})$  by  $I_n(\hat{\theta}_{0,n})$  using Riemann sums to estimate the integrals and to compute the expectations, for instance  $\mathbb{E}(h_{\bar{\alpha}_n}(L_1^{\bar{\alpha}_n}))$ . As the matrix  $I_n(\hat{\theta}_{0,n})$  is full, the resulting Monte-Carlo simulation drastically slows down the estimation. In conclusion, this method would be significantly longer for similar results.

However, this method would be worth considering when working with a symmetric stable process  $S^\alpha$  such as in Brouste and Masuda [BM18]. In this case a lot of terms in the matrix  $I_n(\hat{\theta}_{0,n})$  are 0, leaving us with only a few expectations to compute which makes this technique viable.

## FUNDING

This work was supported by French ANR reference ANR-21-CE40-0021.

## REFERENCES

- [BC23] Elise Bayraktar and Emmanuelle Clément. Estimation of a pure-jump stable Cox-Ingersoll-Ross process. To appear in Bernoulli hal-04037024, March 2023.
- [BM18] Alexandre Brouste and Hiroki Masuda. Efficient estimation of stable Lévy process with symmetric jumps. *Stat. Inference Stoch. Process.*, 21(2):289–307, 2018.
- [CG20] Emmanuelle Clément and Arnaud Gloter. Joint estimation for SDE driven by locally stable Lévy processes. *Electron. J. Stat.*, 14(2):2922–2956, 2020.
- [CIR85] John C. Cox, Jonathan E. Ingersoll, Jr., and Stephen A. Ross. A theory of the term structure of interest rates. *Econometrica*, 53(2):385–407, 1985.
- [FL10] Zongfei Fu and Zenghu Li. Stochastic equations of non-negative processes with jumps. *Stochastic Process. Appl.*, 120(3):306–330, 2010.
- [JMS17] Ying Jiao, Chunhua Ma, and Simone Scotti. Alpha-CIR model with branching processes in sovereign interest rate modeling. *Finance Stoch.*, 21(3):789–813, 2017.
- [JMSZ21] Ying Jiao, Chunhua Ma, Simone Scotti, and Chao Zhou. The alpha-Heston stochastic volatility model. *Math. Finance*, 31(3):943–978, 2021.
- [JP12] Jean Jacod and Philip Protter. *Discretization of processes*, volume 67 of *Stochastic Modelling and Applied Probability*. Springer, Heidelberg, 2012.
- [LM11] Zenghu Li and Leonid Mytnik. Strong solutions for stochastic differential equations with jumps. *Ann. Inst. Henri Poincaré Probab. Stat.*, 47(4):1055–1067, 2011.
- [LT19] Libo Li and Dai Taguchi. On a positivity preserving numerical scheme for jump-extended CIR process: the alpha-stable case. *BIT*, 59(3):747–774, 2019.

- [Mas09] Hiroki Masuda. Joint estimation of discretely observed stable Lévy processes with symmetric Lévy density. *J. Japan Statist. Soc.*, 39(1):49–75, 2009.
- [Mas19] Hiroki Masuda. Non-Gaussian quasi-likelihood estimation of SDE driven by locally stable Lévy process. *Stochastic Process. Appl.*, 129(3):1013–1059, 2019.
- [Mas23] Hiroki Masuda. Optimal stable Ornstein-Uhlenbeck regression. *Jpn. J. Stat. Data Sci.*, 6(1):573–605, 2023.
- [MT06] Muneya Matsui and Akimichi Takemura. Some improvements in numerical evaluation of symmetric stable density and its derivatives. *Comm. Statist. Theory Methods*, 35(1-3):149–172, 2006.
- [Nol97] John P. Nolan. Numerical calculation of stable densities and distribution functions. *Comm. Statist. Stochastic Models*, 13(4):759–774, 1997.
- [Sat13] Ken-iti Sato. *Lévy processes and infinitely divisible distributions*, volume 68 of *Cambridge Studies in Advanced Mathematics*. Cambridge University Press, Cambridge, 2013. Translated from the 1990 Japanese original, Revised edition of the 1999 English translation.
- [Tod13] Viktor Todorov. Power variation from second order differences for pure jump semimartingales. *Stochastic Process. Appl.*, 123(7):2829–2850, 2013.
- [VGO<sup>+</sup>20] Pauli Virtanen, Ralf Gommers, Travis E. Oliphant, Matt Haberland, Tyler Reddy, David Cournapeau, Evgeni Burovski, Pearu Peterson, Warren Weckesser, Jonathan Bright, Stéfan J. van der Walt, Matthew Brett, Joshua Wilson, K. Jarrod Millman, Nikolay Mayorov, Andrew R. J. Nelson, Eric Jones, Robert Kern, Eric Larson, C J Carey, İlhan Polat, Yu Feng, Eric W. Moore, Jake VanderPlas, Denis Laxalde, Josef Perktold, Robert Cimrman, Ian Henriksen, E. A. Quintero, Charles R. Harris, Anne M. Archibald, Antônio H. Ribeiro, Fabian Pedregosa, Paul van Mulbregt, and SciPy 1.0 Contributors. SciPy 1.0: Fundamental Algorithms for Scientific Computing in Python. *Nature Methods*, 17:261–272, 2020.
- [WMctm16] Diethelm Wuertz, Martin Maechler, and Rmetrics core team members. *stabledist: Stable Distribution Functions*, 2016. R package version 0.7-1.
- [WW95] Aleksander Weron and Rafal Weron. Computer simulation of Lévy  $\alpha$ -stable variables and processes. In *Chaos—the interplay between stochastic and deterministic behaviour (Karpacz, 1995)*, volume 457 of *Lecture Notes in Phys.*, pages 379–392. Springer, Berlin, 1995.